



Research article

Inhibition of autophagosome-lysosome fusion contributes to TDCIPP-induced A β 1-42 production in N2a-APPswe cells

Chunli Zou^{a,b,1}, Tingting Yang^{a,b,1}, Xinfeng Huang^b, Xiaohu Ren^b, Chen Yang^b, Benhong Xu^{b,*}, Jianjun Liu^{a,b,**}

^a College of Public Health, Zunyi Medical University, Zunyi, 563000, China

^b Shenzhen Key Laboratory of Modern Toxicology, Shenzhen Medical Key Discipline of Health Toxicology, Shenzhen Center for Disease Control and Prevention, Shenzhen, 518000, China

ARTICLE INFO

Keywords:

Alzheimer's disease
TDCIPP
Autophagy
A β 42

ABSTRACT

Alzheimer's disease is the most common form of dementia and is characterized by cognitive impairment. The disruption of autophagosome-lysosome function has been linked to the pathogenesis of Alzheimer's disease. Tris (1,3-dichloro-2-propyl) phosphate (TDCIPP) is a widely used organophosphorus flame retardant that has the potential to cause neuronal damage. We found that TDCIPP significantly increased the expression of β -site amyloid precursor protein (APP)-cleaving enzyme 1 (BACE1), presenilin-1 (PS1) and A β 42. Proteomic studies with TMT labeling revealed changes in the profiles of N2a-APPswe cells after exposure to TDCIPP. Proteomic and bioinformatics analyses revealed that lysosomal proteins were dysregulated in N2a-APPswe cells after treatment with TDCIPP. The LC3, P62, CTSD, and LAMP1 levels were increased after TDCIPP exposure, and dysregulated protein expression was validated by Western blotting. The exposure to TDCIPP led to the accumulation of autophagosomes, and this phenomenon was enhanced in the presence of chloroquine (CQ). Our results revealed for the first time that TDCIPP could be a potential environmental risk factor for AD development. The inhibition of autophagosome-lysosome fusion may have a significant impact on the generation of A β 1-42 in response to TDCIPP.

1. Introduction

Alzheimer's disease (AD) is the most common form of dementia and is characterized by progressive neuronal loss and cognitive impairment [1]. It is estimated that 152 million people will suffer from dementia by 2050 [2]. Thus, AD is a growing public health problem worldwide. The two pathological hallmarks in the brains of patients with AD are extracellular senile plaques that are composed of amyloid β peptide (A β) and intracellular neurofibrillary tangles (NFTs) that are composed of hyperphosphorylated tau proteins [3,4]. However, the causes of sporadic cases AD are unknown. There has been growing interest in the relationship between exposure to environmental pollutants and the development of AD.

Organophosphorus flame retardants (OPFRs) are widely used in various industries due to their excellent performance in reducing

* Corresponding author.

** Corresponding author.

E-mail addresses: xubenhong@szcdc.net (B. Xu), toxic_01@szcdc.net (J. Liu).

¹ These authors have contributed equally to this work.

polymer flammability or increasing polymer plasticity [5,6]. The use of OPFRs has been reported to be rapidly increasing in recent years, and OPFRs have become a new type of pollutant in the environment and air [7–9]. Recent studies have shown that skin contact and dust inhalation are the main routes of exposure to OPFRs in the general population and that OPFRs can accumulate in the human body [10]. A variety of body systems, including the endocrine system, reproductive system, and nervous system [11–14], can be damaged by OPFR exposure.

Tris(1,3-dichloro-2-propyl) phosphate (TDCIPP) is a widely used organophosphorus flame retardant that is found in environmental media and biota, including humans [15]. Exposure to TDCIPP can cause axonal and cholinergic neuronal damage as well as vascular and muscle development disorders in zebrafish [16,17]. TDCIPP exposure significantly increases autophagy in the nervous system of zebrafish [18]. TDCIPP triggers autophagy and promotes the differentiation of SH-SY5Y cells [19]. We previously reported that there exists a positive correlation between urinary levels of BDCIPP and decreased cognitive abilities [20], and we also found that TDCIPP induced cognitive impairment in rats [21]. Disruptions in the lysosomal autophagic process are one of the main causes of the accumulation of proteins that are associated with AD pathology [22]. However, the relationship between TDCIPP exposure and AD development has rarely been reported and is not currently clear.

In this study, we used a combined quantitative proteomics and bioinformatics approach to investigate the differences in cellular proteome expression and protein molecular regulatory networks in N2a-APPswe cells after TDCIPP treatment. Our study revealed that TDCIPP exposure could be a risk factor for the pathological progression of AD.

2. Materials and methods

2.1. Chemicals and reagents

Tris(1,3-dichloro-2-propyl) phosphate (TDCIPP) (98% purity) was purchased from Macklin Reagent (Shanghai, China). Chloroquine (CQ) (97% purity) was purchased from MedChemExpress (Shanghai, China) and used here as an autophagy inhibitor. Tandem mass tag (TMT)-labeling kits were purchased from Thermo Scientific (NJ, USA). Sequencing-grade trypsin/Lys-C mix mixtures were purchased from Promega (WI, USA). Human A β 1-42 (amyloid beta 1–42) ELISA kits were purchased from Elabscience (Wuhan, China). CYTO-ID® Autophagy Detection kit purchased from Enzo Life Sciences (NY, USA). Tricine-SDS-PAGE Gel Preparation kits were purchased from Sangon Biotech (Shanghai, China). Anti-presenilin-1 (anti-PS1, AF0245) was purchased from Affinity Bioscience (Jiangsu, China). Anti-LC3 (12741T) and anti-BACE1 (5606S) antibodies were purchased from Cell Signaling Technology (MA, USA). Anti-P62 (ab109012), anti-CTSD (ab6313), and anti-LAMP1 (ab24170) antibodies were purchased from Abcam (Cambridge, UK).

2.2. Cell culture

N2a-WT (WT) and N2a-APPswe cells were kindly donated by Professor Jian-zhi Wang (Tongji Medical School, China). N2a-APPswe cells were cultured in mixed medium containing DMEM and OPTI-MEM (1:1 (v/v)) supplemented with 10% (v/v) fetal bovine serum (FBS) and 200 μ g/mL G418. N2a-WT cells were cultured in complete DMEM supplemented with 10% (v/v) FBS. All the cells were cultured in a humidified incubator at 37 °C in 5% CO₂.

2.3. TDCIPP treatment of N2a-APPswe cells

Stock solutions of CQ and TDCIPP were dissolved in DMSO and diluted with cell culture medium to the desired final concentrations. The cells were subjected to incubation with 15 μ M TDCIPP, 45 μ M TDCIPP with or without 50 μ M CQ, and 50 μ M CQ individually for a duration of 24 h. DMSO was employed as the vehicle control. Then the cells and cell culture medium were separately collected for subsequent analysis.

2.4. TMT labeling

After incubation with TDCIPP or solvent control, the cells were lysed with 8 M urea and disrupted using sonication. Proteins were collected after centrifugation at 12000 rpm for 10 min at 4 °C. Quantification of protein concentrations was carried out using the BCA Protein Assay Kit (23225, Thermo Fisher Scientific). Fifty micrograms of protein from each group was used for subsequent TMT labeling as we previously reported [23]. Briefly, 10 mM dithiothreitol (DTT) was added to each sample and incubated for 1 h at 37 °C, and 25 mM 2-iodoacetamide (IAA) was added and incubated for 1 h in the dark at room temperature. Trypsin/Lys-C Mix was added to a protein at a 25:1 protein:protease ratio (w/w) and incubated at 37 °C for 12 h. An Oasis HLB column cartridge (Waters, MC, USA) was used for desalting. Then, the samples were redissolved in 100 μ L triethylammonium bicarbonate buffer (TEAB, 200 mM, pH 8.5) and labeled with TMT as follows: TMT-126, N2a-WT cells; TMT-127, N2a-APPswe cells (Vehicle control); TMT-128, N2a-APPswe cells treated with 15 μ M TDCIPP; and TMT-129, N2a-APPswe cells treated with 45 μ M TDCIPP.

2.5. LC-MS/MS analysis

Each fraction was separated with a silica capillary column (75 μ l internal diameter (ID), 150 mm length; Upchurch, Oak Harbor, WA, USA) that was packed with C18 resin (300 Å, 5 μ l; Varian, Lexington, MA, USA) and then analyzed with an Orbitrap Exploris™ 480 mass spectrometer (Thermo Scientific, NJ, USA). The data-dependent acquisition (DDA) mode was used, and full scans in the

Orbitrap mass analyzer (350-1, 500 *m/z*, 120,000 resolution) were followed by data-dependent MS/MS scans. The scan range mode was used to define the first mass (110 *m/z*). MS/MS spectra were searched using SEQUEST search algorithms embedded in Proteome Discoverer 2.5 (Thermo Scientific) against the UniProt_mouse database (downloaded from the UniProt database on March 22, 2023). The search parameters were set to default with modifications. The enzyme was set to trypsin, and two missed cleavage sites were allowed. Carbamidomethylation (C, +57.021 Da) was set as the static modification. TMT6-plex (lysine [K] and any N-terminal of peptides) and oxidation (methionine, M) were used as dynamic modifications as previously reported. Changes in proteins were evaluated by the comparison of reporter ions from each group.

2.6. Bioinformatics analysis

All the protein abundances were input into Rstudio software for analysis. Heatmaps were generated using TBtools software, and volcano maps were generated using GraphPad software. Kyoto Encyclopedia of Genes and Genomes (KEGG) pathway analysis and gene ontology (GO) analysis of all the differentially expressed proteins were performed using the DAVID database (<https://david.ncifcrf.gov/>).

2.7. Immunofluorescence staining

N2a-APPswe cells were treated with TDCIPP or CQ for a duration of 24 h, then cells were fixed with 4% paraformaldehyde for 20 min and permeabilized with 0.2% Triton-100 for another 20 min. The cells were incubated with LC3 or P62 antibodies at 4 °C overnight. Cells were incubated with Alexa Fluor® 488-coupled goat anti-rabbit IgG secondary antibody for 1 h at room temperature,

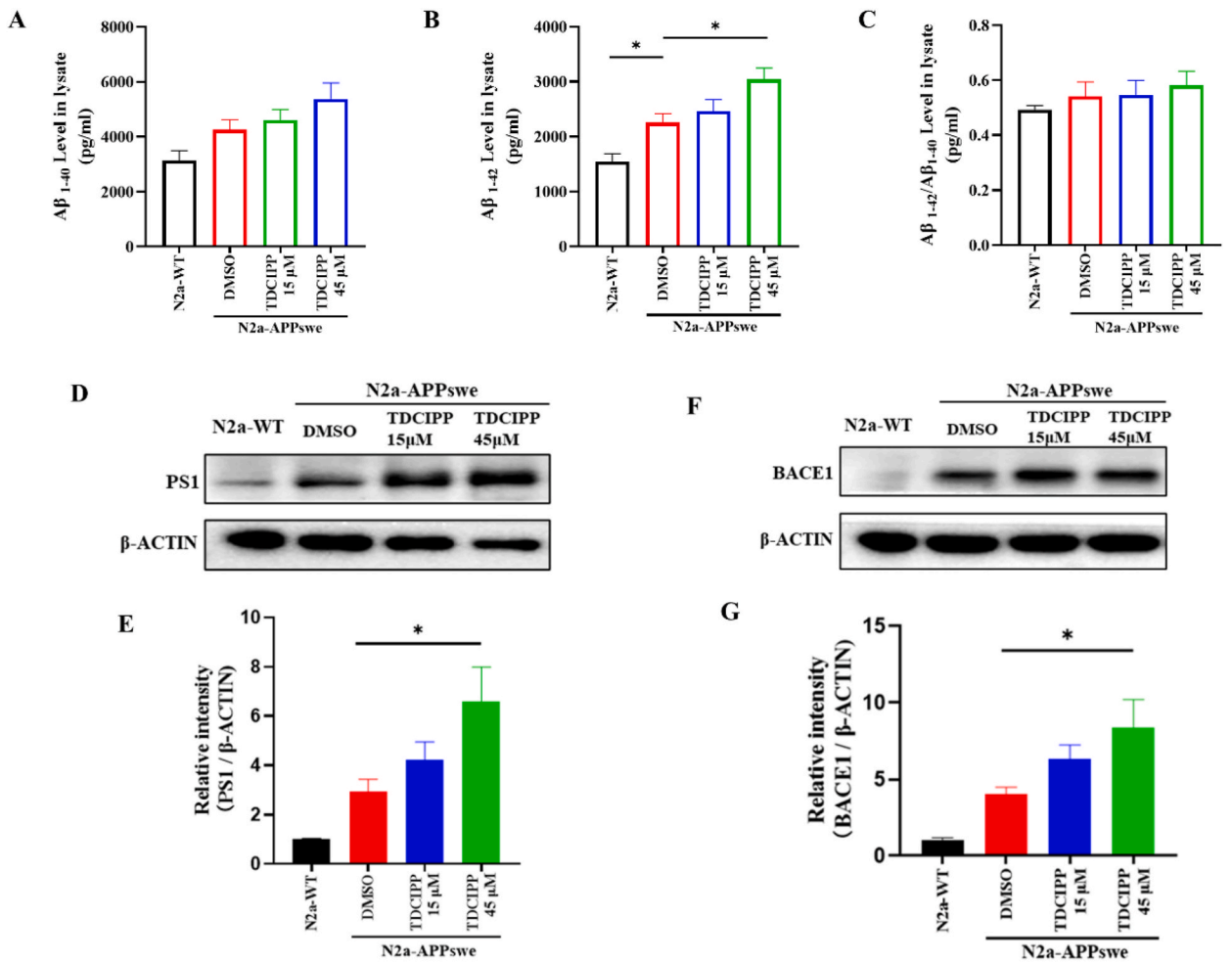


Fig. 1. TDCIPP promotes the production of Aβ₁₋₄₂. (A) Human Aβ₁₋₄₀ (Amyloid Beta 1–40) ELISA Kit was used to detect the expression level of Aβ₁₋₄₀. (B) Human Aβ₁₋₄₂ (Amyloid Beta 1–42) ELISA Kit was used to detect the expression level of Aβ₁₋₄₂. (C) Ratio of Aβ₁₋₄₂ to Aβ₁₋₄₀ was calculated based on levels of Aβ₁₋₄₂ and Aβ₁₋₄₀. (D–E) Western blot analysis and quantification of PS1 expression levels. (F–G) Western blot analysis and quantification of BACE1 expression levels. Data are shown as mean ± SEM. *, p < 0.05, **, p < 0.01.

and then were washed with PBS and stained with DAPI for 3 min. Images were obtained by a confocal microscopy (ZEISS, LSM980). The images were quantitatively evaluated by the ImageJ software.

2.8. ENZO CYTO-ID® kit for autophagy detection

The cells were treated with TDCIPP at concentrations of 15 μM or 45 μM , chloroquine at a concentration of 50 μM , or a combination of TDCIPP at 45 μM and chloroquine at 50 μM for 24 h. DMSO was employed as the vehicle control. Cells were washed with phosphate-buffered and fixed with 4% paraformaldehyde for 20 min. Subsequently, the cells were stained with the CYTO-ID® autophagic green dye for 30 min at an incubation temperature of 37 $^{\circ}\text{C}$, and then rinsed with buffer before being stained with DAPI for 3 min. The resulting images were captured using a confocal microscopy system (ZEISS, LSM980). The acquired images were quantitatively evaluated using the ImageJ software.

2.9. Measurement of Human A β 1-42 (amyloid beta 1–42) levels by ELISA

The concentration of A β 1-42 was measured with a double antibody sandwich ELISA kit. One hundred microliters of standard or sample was added to a 96-well plate and incubated at 37 $^{\circ}\text{C}$ for 90 min. The liquid in the wells was removed, and 100 μL of biotinylated antibody added and incubated at 37 $^{\circ}\text{C}$ for 60 min. The wells were washed 3 times with washing solution, 100 μL of enzyme conjugate working solution added and incubated at 37 $^{\circ}\text{C}$ for 30 min, and the plate was washed 6 times. Then, 90 μL of substrate solution was added to the wells and incubated at 37 $^{\circ}\text{C}$ for 15 min. Fifty microliters of termination solution were added, and the OD was immediately measured at 450 nm.

3. Western blotting analysis

After protein quantitation and denaturation, the protein samples were subsequently loaded onto 10% or 12% polyacrylamide gels. After electrophoresis, the proteins were transferred to PVDF membranes, which were then blocked with 5% nonfat milk powder dissolved in TBST for 90 min. Primary antibodies (anti-LC3, anti-P62, anti-CTSD, anti-LAMP1, anti-PS1 and anti-BACE1 antibodies) were added and incubated overnight in a shaker at 4 $^{\circ}\text{C}$, followed by three washes with TBST for 10 min each and incubation with secondary antibodies for 1 h. Background removal solution was used for membrane exposure, and bands were captured and analyzed with a multifunctional imager (Cytiva, MA, USA).

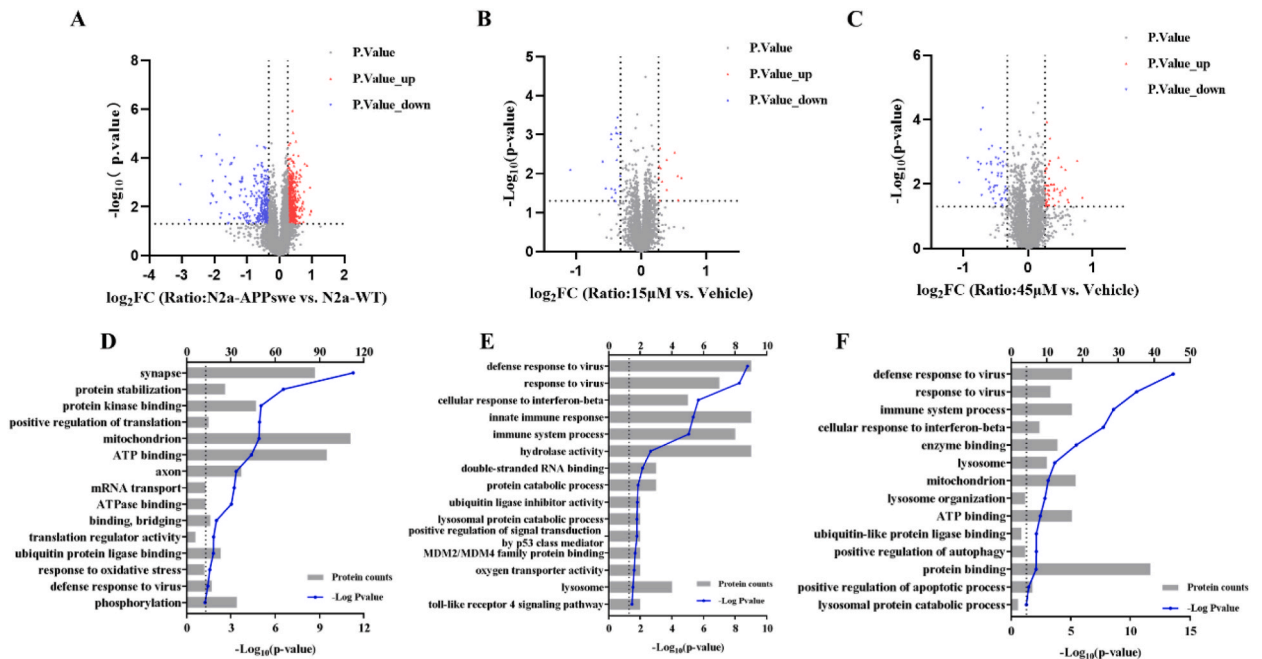


Fig. 2. Volcano map and Gene ontology enrichment analysis of differentially expressed proteins. (A) Dysregulated proteins in the N2a-APPswe group compared with N2a-WT. (B) Dysregulated proteins in 15 μM TDCIPP-treated N2a-APPswe cells compared with that of vehicle control. (C) Dysregulated proteins of 45 μM TDCIPP-treated N2a-APPswe cells compared with that of vehicle control. Red dots indicate significantly upregulated proteins and blue dots represent downregulated proteins. (D) GO analysis of differentially expressed proteins in the N2a-APPswe vs. WT group. (E) GO analysis of differentially expressed proteins in the 15 μM vs. N2a-APPswe TDCIPP treatment group. (F) GO analysis of differentially expressed proteins in the 45 μM vs. N2a-APPswe TDCIPP-treated group. (For interpretation of the references to colour in this figure legend, the reader is referred to the Web version of this article.)

4. Results

4.1. TDCIPP increases A β 1-42 production

Exposure of N2a-APPsw cells to TDCIPP for 24 h results in a concentration-dependent increase in A β levels (Fig. 1A and B) and neurotoxicity (Fig. S1). The 15 μ M TDCIPP treatment group exhibited increased expression of A β 1-42 compared to the vehicle-treated group ($p > 0.05$). The 45 μ M TDCIPP treatment group exhibited significantly increased expression of A β 1-42 ($p < 0.05$) (Fig. 1B). TDCIPP treatment increased ratio of A β 1-42/A β 1-40, but without significant difference ($p > 0.05$) (Fig. 1C).

Both presenilin-1 (PS1) and beta-site APP-cleaving enzyme 1 (BACE1) are important for the production of A β 40 and A β 42 [24,25]. The protein level of PS1 exhibited a significant increase ($P < 0.05$) in the group treated with 45 μ M TDCIPP in comparison to the N2a-APPsw cells treated with the vehicle. (Fig. 1D–E). The protein level of BACE1 was significantly upregulated ($P < 0.05$) in the 45 μ M TDCIPP-treated group compared with that in the vehicle-treated N2a-APPsw cells (Fig. 1F–G). No statistically significant disparity was observed in the protein expression levels of APP, ADAM10, and IDE between the TDCIPP-treated group and the DMSO-treated group (Fig. S2).

4.2. Hundreds of proteins were dysregulated after TDCIPP treatment

To evaluate the potential role of TDCIPP in AD development, a proteomic study with TMT labeling was performed using N2a-APPsw cells. In total, 6220 proteins were identified and quantified by mass spectrometry, with a false discovery rate (FDR) less than 1%. Compared with the N2a-WT group, 827 proteins were dysregulated in the N2a-APPsw group, of which 545 were upregulated and 282 were downregulated (Fig. 2A). Compared with the N2a-APPsw group, the 15 μ M TDCIPP treatment group had 31 differentially expressed proteins, of which there were 12 upregulated and 19 downregulated proteins (Fig. 2B). Compared with the N2a-APPsw group, the 45 μ M TDCIPP treatment group had 97 differentially expressed proteins, including 49 upregulated and 48 downregulated proteins (Fig. 2C).

To understand the function of the dysregulated proteins, GO enrichment analysis was performed. Compared to the N2a-WT cells, the differentially expressed proteins in the N2a-APPsw cells were mainly enriched in protein stabilization, defense response to virus, and autophagy (Fig. 2D). In N2a-APPsw cells, compared with the DMSO-treated group, differentially expressed proteins in the 15 μ M

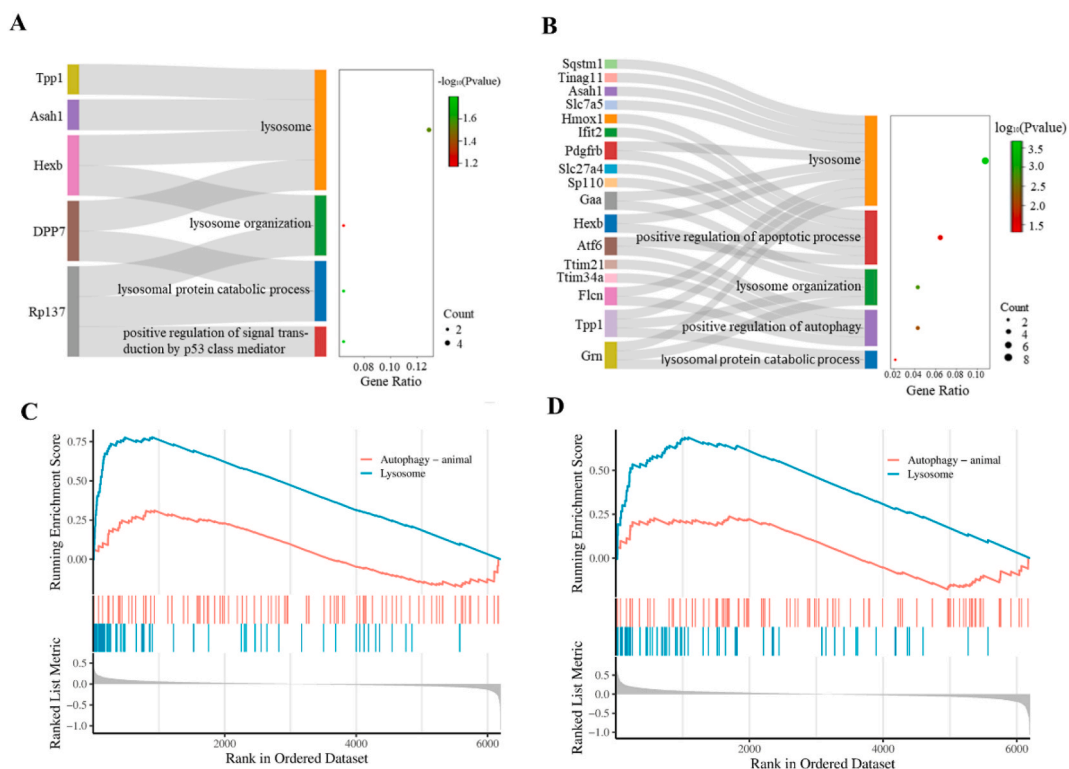


Fig. 3. Sankey and GSEA map analysis for the changed proteins of 15 μ M TDCIPP-treated group and 45 μ M TDCIPP-treated group. (A) Sang motif maps of the 15 μ M TDCIPP-treated group and (B) 45 μ M TDCIPP-treated group were analyzed using the DIVID database. (C–D) GSEA used clusterprofiler R package for gene set enrichment analysis, and KEGG datasets were obtained from the GSEA official website. The bar codes indicate the encountered proteins in the pivotal pathways.

TDCIPP treatment group were mainly enriched in the defense response to virus and positive regulation of signal transduction by p53 and lysosomes (Fig. 2E). The differentially expressed proteins in the 45 μ M TDCIPP treatment group were mainly enriched in the defense response to virus, lysosome organization, and positive regulation of autophagy (Fig. 2F). GO analysis showed that the dysregulated proteins after TDCIPP treatment were related with lysosomal and autophagic regulation.

4.3. Sankey and gene set enrichment analysis (GSEA) of autophagy-lysosome-associated proteins that were differentially expressed after TDCIPP treatment

The dysregulated proteins from GO annotation on autophagy-lysosome-related pathways were subjected to Sankey and GSEA. In the 15 μ M TDCIPP-treatment group, lysosome, lysosome organization, lysosomal protein catabolic process and the positive regulatory role of lysosomal p53-like mediators in signal transduction were enriched for the dysregulated proteins. These proteins included TPP1, ASAH1, HEXB, DPP7, and RPL37. (Fig. 3A and Table 1). The dysregulated proteins in the 45 μ M TDCIPP-treatment group exhibited enrichment in various cellular processes, including lysosome organization, positive regulation of apoptotic process, positive regulation of autophagy, and lysosomal protein catabolic process, as depicted in Fig. 3B. The detailed changed proteins are also listed in Table 2. GSEA revealed that the autophagy-lysosome pathway was gradually activated after TDCIPP treatment, and the corresponding running enrichment scores are shown in Fig. 3C–D.

4.4. TDCIPP inhibits autophagosome-lysosome fusion

To examine the correlation between TDCIPP and autophagy on N2a-APPswe cells, we examined the protein expression level of LC3. As shown in Fig. 4A–B, it was observed that treatment with 45 μ M TDCIPP increased levels of LC3 compared with that of the vehicle-treated group ($p < 0.01$). Compared with the 45 μ M TDCIPP-treated group, LC3 levels were significantly higher in the TDCIPP-combined-CQ treatment group ($p < 0.001$). The accumulation of P62 serves as an indicator of impeded or suppressed autophagic flux [26]. P62 levels were significantly elevated in the 45 μ M TDCIPP-treated group compared to that of the vehicle-treated group (Fig. 4C–D). To further confirm the association between TDCIPP and autophagy, the ENZO CYTO-ID® Kit was employed to assess the autophagic flux. The findings demonstrate that TDCIPP notably promotes the accumulation of autophagosomes in comparison to the control group. Moreover, the inhibitory impact of CQ on lysosomes was augmented when CQ and TDCIPP were administered in combination (Fig. 4E–F).

4.5. Heatmap and western blotting analysis demonstrated that TDCIPP inhibits autophagy and led to an increase in lysosome levels

Heatmap analysis is employed to visually represent variations in protein expression among distinct treatment groups (Fig. 5A). According to the autophagy expression profile, we found that most of the proteins, including SQSTM1 (P62), GRN and other proteins, were upregulated after treatment with 45 μ M TDCIPP. According to the lysosomal expression profile, we found that all the differentially expressed proteins, including FLCN, ASAH1 and other proteins, were upregulated after treatment with 45 μ M TDCIPP (Fig. 5A).

To further validate the dysregulated proteins that were identified in the proteomic study, Western blotting analysis was performed to measure microtubule-associated protein LC3, P62, lysosome-associated membrane glycoprotein 1 (LAMP1) and cathepsin D (CTSD) expression. The protein level of LC3II was significantly upregulated ($P < 0.01$) in the 45 μ M TDCIPP-treated group compared with that in the vehicle-treated N2a-APPswe cells. Compared with the 45 μ M TDCIPP-treated group, LC3II expression was significantly increased in the TDCIPP + CQ treatment group ($P < 0.01$) (Fig. 5B and Fig. S4). P62 was significantly increased in the 15 μ M and 45 μ M TDCIPP-treatment group compared with the vehicle group ($P < 0.01$) and further increased after CQ treatment ($P < 0.05$), indicating that the autophagy was inhibited when exposed to TDCIPP (Fig. 5B and Fig. S4). We assessed the protein levels of the lysosomal markers LAMP1 and CTSD to assess whether the downstream autophagic process was disrupted. The levels of CTSD were found to be significantly higher in the group treated with 45 μ M TDCIPP compared to the vehicle group ($P < 0.001$). Additionally, the treatment of N2a-APPswe cells with 45 μ M TDCIPP resulted in an increase in LAMP1 levels compared to the vehicle-treated cells ($P < 0.05$) (Fig. 5B, Figs. S3 and S4). In summary, the results of Western blotting analysis were consistent with the proteomic data.

5. Discussion

AD is an irreversible neurodegenerative brain disease that is characterized by neuritic plaques that are composed of extracellular

Table 1
Autophagy-lysosome-associated protein changes in the 15 μ M TDCIPP-treated group.

Uniprot-AC	Gene Name	P.Value	Log ₂ FC
Q9WV54	Asah1	0.02	0.32
Q9ET22	Dpp7	0.01	0.30
O89023	Tpp1	0.05	0.28
P20060	Hexb	0.01	0.27
Q9D823	Rpl37	0.02	-0.55

Table 2
Autophagy-lysosome-associated protein changes in the 45 μ M TDCIPP-treated group.

AC-uniprot	gene name	P.Value	Log ₂ FC
P14901	Hmox1	<0.01	0.58
Q9WV54	Asah1	<0.01	0.52
F6VAN0	Atf6	0.01	0.40
P70699	Gaa	<0.01	0.32
Q64337	Sqstm1	<0.01	0.32
P20060	Hexb	0.01	0.31
P28798	Grn	0.02	0.31
Q99JR5	Tinag1	0.01	0.29
O89023	Tpp1	0.04	0.28
Q9Z127	Slc7a5	0.04	0.27
P05622	Pdgfrb	0.02	0.27
Q91VE0	Slc27a4	0.02	0.26
Q8QZS3	Flcn	0.01	0.26
Q8BVK9	Sp110	<0.01	-0.33
Q62191	Trim21	0.02	-0.35
Q99PP6	Trim34a	0.01	-0.61
Q64112	lfit2	<0.01	-0.93

aggregates of amyloid β (A β) peptides; these plaques are one of the main pathological features of AD. TDCIPP is an emerging environmental pollutant that exerts neurotoxic effects. In this study, we used proteomics and Western blotting to reveal proteomic changes in N2A-APP_{swe} cells after TDCIPP treatment. Our research discovered that treatment of N2a-APP_{swe} cells with TDCIPP resulted in the inhibition of autophagosome-lysosome fusion. The upregulation of lysosome-associated proteins CTSD and LAMP1, which may lead to lysosomal dysfunction, results in elevated A β 1-42 levels, thereby promoting the development of AD.

Autophagy refers to the degradation and recirculation of cellular materials through the lysosomal pathway, and lysosomes are essential for the autophagic mechanism [27]. Mammalian target of rapamycin (mTOR) is a serine/threonine protein kinase [28]. mTOR signaling is a central regulator of autophagy, and it regulates multiple aspects of autophagy initiation, process and termination by controlling unc51-like kinase 1 (ULK1) complex activity as well as proto-lysosome tubule reformation [29]. mTOR and STAT1 are mutually regulated, and a physical association between mTOR and STAT1 has been shown in human cells [30,31]. Signal transducer and activator of transcription 1 (STAT1) is a nuclear transcription factor that is involved in the regulation of genes that are related to cell survival, the cell cycle and immune responses [32]. STAT1 can negatively regulate ULK1 expression and autophagy [33]. Recent studies have shown that hair cells in STAT1-deficient mice exhibit enhanced autophagic flux [34]. In the skeletal muscle of stat1-deficient mice, ULK1 protein levels and autophagic flux are significantly enhanced. In STAT1-deficient human fibrosarcoma cells, *stat1* is regulated by mTOR to enhance the autophagic flux [33]. In proteomic analysis, STAT1 expression was decreased in a concentration-dependent manner after TDCIPP treatment, which enhanced autophagosome formation. Furthermore, our findings indicate that the administration of TDCIPP resulted in an upregulation of P62 expression, implying a disturbance in the process of autophagic degradation in response to TDCIPP.

The autophagy-lysosome pathway plays a key role in the quality of cellular components and cellular homeostasis, and its dysfunction can lead to the neuronal cell death that is associated with various neurodegenerative diseases [35], including AD; thus, dysfunction of the autophagy-lysosome pathway contributes to the pathogenesis of neurodegenerative diseases [36]. Studies of cerebrospinal fluid from AD patients have shown elevated concentrations of the lysosome-associated proteins CTSD, LAMP1 and LAMP2 [37]. Studies on neuronal cells show that lysosomal dysfunction contributes to the proliferation of the pathological marker proteins A β and tau in AD [38–40]. In the present study, TDCIPP induced the expression of the lysosomal proteins CTSD and LAMP1. Treatment with TDCIPP resulted in disruption of autophagic flux, resembling the effects induced by CQ, a well-known inhibitor of lysosome and autophagy. Our proteomic findings, in conjunction with these observations, indicate that TDCIPP inhibits autophagosome-lysosome fusion. The observed upregulation of lysosome proteins may be a compensatory response to the inhibition of autophagosome-lysosome fusion, warranting further investigation. It is worth noting that the inhibition of autophagosome-lysosome fusion could potentially lead to an increase in A β protein production, thereby posing a potential threat to neuronal cells.

6. Conclusions

In conclusion, our study showed for the first time that TDCIPP can induce A β 1-42 production through the autophagy-lysosomal pathway and thus is associated with the development of AD. TDCIPP promotes the accumulation of autophagosomes and inhibits autophagosome-lysosome fusion. In addition to this study, further mechanisms need to be explored, especially those related to autophagy-lysosome function, through in vivo experiments.

Data availability statement

The mass spectrometry proteomics data have been deposited in the ProteomeXchange Consortium via the PRIDE partner repository with the dataset identifier PXD042789 and 10.6019/PXD042789.

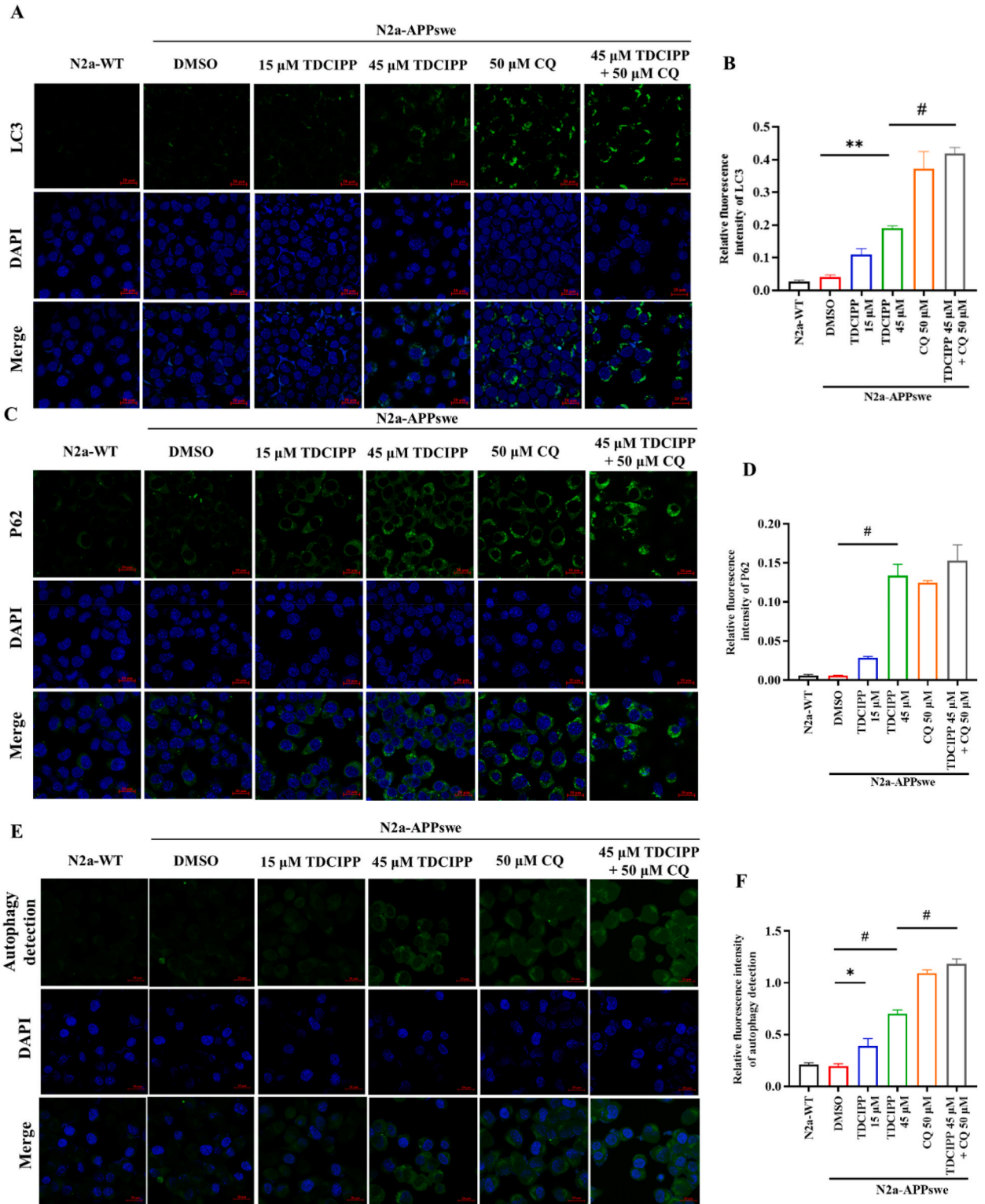


Fig. 4. Treatment with TDCIPP results in the aggregation of autophagosomes in N2a-APPswe cells. Cellular immunofluorescence was conducted along with statistical analysis to examine the expression of LC3 (A–B) and P62 (C–D). Cellular immunofluorescence and statistical analysis for autophagy detection (E–F). Scale bar = 20 μ m. The data are expressed as the mean \pm SEM; * P < 0.05, ** P < 0.01, # P < 0.001.

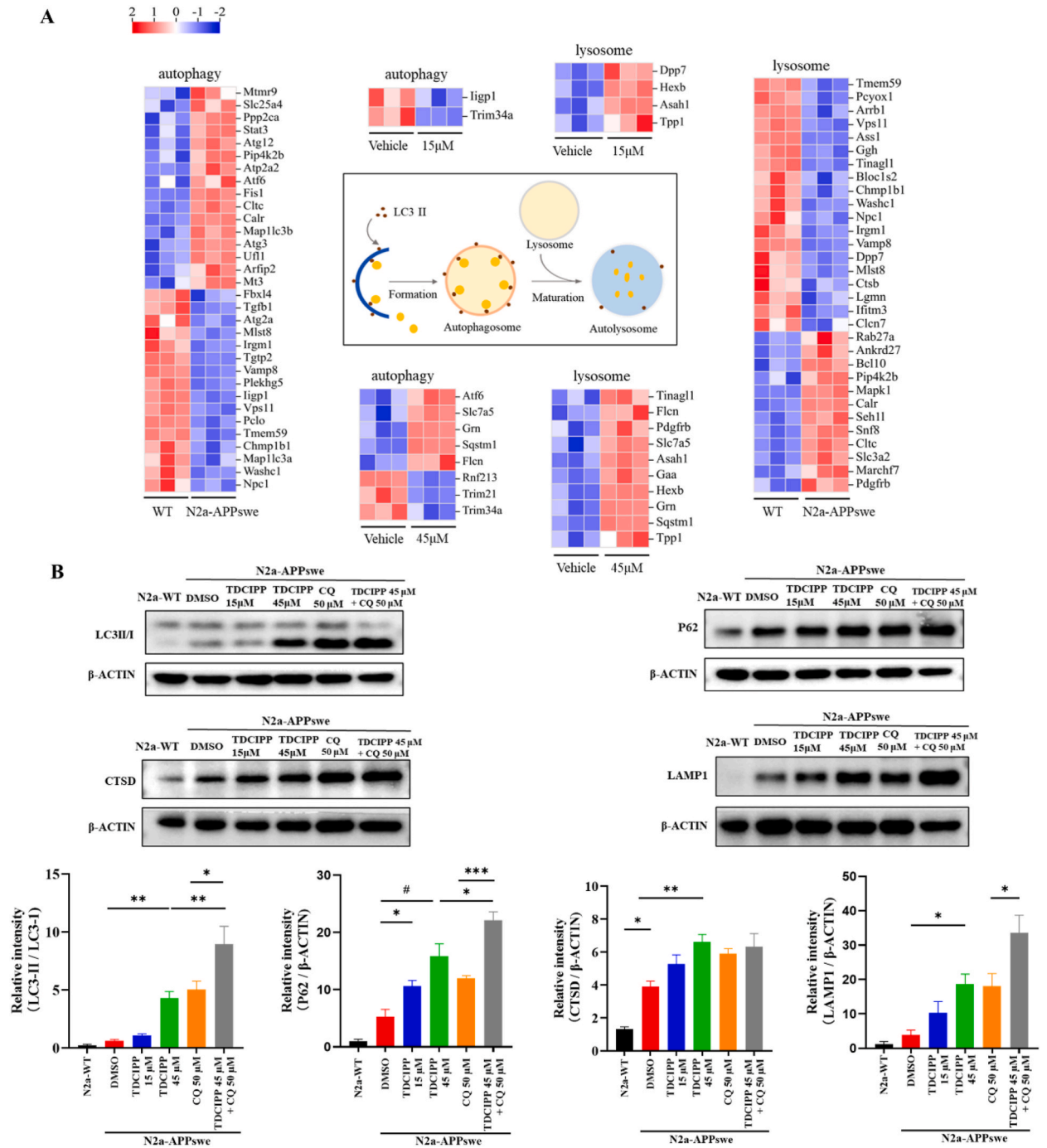


Fig. 5. TDCIPP inhibits autophagy and led to an increase in lysosome levels. (A) Differential proteins located in autophagy and lysosomes were localized according to GO annotation and Uniprot database. The heat map is clustered in rows, with blue representing down-regulated proteins and red up-regulated proteins. (B) Western blot analysis and quantification of LC3, P62, CTSD, LAMP1 expression levels. Data are shown as Mean ± SEM. *, $p < 0.05$, **, $p < 0.01$, ***, $p < 0.001$, # $p < 0.0001$. (For interpretation of the references to colour in this figure legend, the reader is referred to the Web version of this article.)

CRedit authorship contribution statement

Chunli Zou: Writing – original draft, Software, Investigation, Data curation. **Tingting Yang:** Writing – original draft, Investigation, Data curation. **Xinfeng Huang:** Writing – review & editing, Project administration. **Xiaohu Ren:** Writing – review & editing,

Methodology. **Chen Yang:** Writing – review & editing, Methodology. **Benhong Xu:** Writing – review & editing, Supervision, Funding acquisition, Conceptualization. **Jianjun Liu:** Writing – review & editing, Funding acquisition, Conceptualization.

Declaration of competing interest

The authors declare that they have no known competing financial interests or personal relationships that could have appeared to influence the work reported in this paper.

Acknowledgment

This project was supported by Shenzhen Science and Technology Program (JCYJ20220530172608018), the Guangdong Natural Science Foundation (2023A1515011983), Shenzhen Medical Research Funding (B2303006), Sanming Project of Medicine in Shenzhen (SZSM202211010), Shenzhen Key Medical Discipline Construction Fund (SZXK069).

Appendix A. Supplementary data

Supplementary data to this article can be found online at <https://doi.org/10.1016/j.heliyon.2024.e26832>.

References

- [1] Q. Yin, X. Ji, R. Lv, J.-J. Pei, Y. Du, C. Shen, et al., Targetting exosomes as a new biomarker and therapeutic approach for Alzheimer's disease, *Clin. Interv. Aging* 15 (2020) 195–205, <https://doi.org/10.2147/CIA.S240400>.
- [2] C. Patterson, *World Alzheimer Report 2018 - the state of the art of dementia research*, *NEW FRONTIERS* (2018) 1–48.
- [3] M.G. Ulep, S.K. Saraon, S. McLea, Alzheimer disease, *J. Nurse Pract.* 14 (2018) 129–135, <https://doi.org/10.1016/j.nurpra.2017.10.014>.
- [4] L. Wang, MicroRNA-200a-3p mediates neuroprotection in alzheimer-related deficits and attenuates amyloid-beta overproduction and tau hyperphosphorylation via coregulating BACE1 and PRKACB, *Front. Pharmacol.* 10 (2019) 12.
- [5] I. Pantelaki, D. Voutsas, Organophosphate flame retardants (OPFRs): a review on analytical methods and occurrence in wastewater and aquatic environment, *Sci. Total Environ.* 649 (2019) 247–263, <https://doi.org/10.1016/j.scitotenv.2018.08.286>.
- [6] J. Huang, Z. Gao, G. Hu, G. Su, Non-target screening and risk assessment of organophosphate esters (OPEs) in drinking water resource water, surface water, groundwater, and seawater, *Environ. Int.* 168 (2022) 107443, <https://doi.org/10.1016/j.envint.2022.107443>.
- [7] Z. Hu, L. Yin, X. Wen, C. Jiang, Y. Long, J. Zhang, et al., Organophosphate esters in China: fate, occurrence, and human exposure, *Toxics* 9 (2021) 310, <https://doi.org/10.3390/toxics9110310>.
- [8] S. Li, F. Zhu, D. Zhang, C. Li, Y. Xu, D. Qing, et al., Seasonal concentration variation and potential influencing factors of organophosphorus flame retardants in a wastewater treatment plant, *Environ. Res.* 199 (2021) 111318, <https://doi.org/10.1016/j.envres.2021.111318>.
- [9] S. Zhao, L. Tian, Z. Zou, X. Liu, G. Zhong, Y. Mo, et al., Probing legacy and alternative flame retardants in the air of Chinese cities, *Environ. Sci. Technol.* 55 (2021) 9450–9459, <https://doi.org/10.1021/acs.est.0c07367>.
- [10] Y. Wang, M. Yang, F. Wang, X. Chen, M. Wu, J. Ma, Organophosphate esters in indoor environment and metabolites in human urine collected from a Shanghai university, *Int. J. Environ. Res. Publ. Health* 18 (2021) 9212, <https://doi.org/10.3390/ijerph18179212>.
- [11] G. Lee, S. Kim, M. Bastiaensen, G. Malarvannan, G. Poma, N. Caballero Casero, et al., Exposure to organophosphate esters, phthalates, and alternative plasticizers in association with uterine fibroids, *Environ. Res.* 189 (2020) 109874, <https://doi.org/10.1016/j.envres.2020.109874>.
- [12] Y. Liu, Y. Li, S. Dong, L. Han, R. Guo, Y. Fu, et al., The risk and impact of organophosphate esters on the development of female-specific cancers: comparative analysis of patients with benign and malignant tumors, *J. Hazard Mater.* 404 (2021) 124020, <https://doi.org/10.1016/j.jhazmat.2020.124020>.
- [13] J.-Y. Zhao, Z.-X. Zhan, M.-J. Lu, F.-B. Tao, D. Wu, H. Gao, A systematic scoping review of epidemiological studies on the association between organophosphate flame retardants and neurotoxicity, *Ecotoxicol. Environ. Saf.* 243 (2022) 113973, <https://doi.org/10.1016/j.ecoenv.2022.113973>.
- [14] L. Sun, W. Xu, T. Peng, H. Chen, L. Ren, H. Tan, et al., Developmental exposure of zebrafish larvae to organophosphate flame retardants causes neurotoxicity, *Neurotoxicol. Teratol.* 55 (2016) 16–22, <https://doi.org/10.1016/j.ntt.2016.03.003>.
- [15] C. Wang, H. Chen, H. Li, J. Yu, X. Wang, Y. Liu, Review of emerging contaminant tris(1,3-dichloro-2-propyl)phosphate: environmental occurrence, exposure, and risks to organisms and human health, *Environ. Int.* 143 (2020) 105946, <https://doi.org/10.1016/j.envint.2020.105946>.
- [16] P.D. Noyes, D.E. Haggard, G.D. Gonnerman, R.L. Tanguay, Advanced morphological - behavioral test platform reveals neurodevelopmental defects in embryonic zebrafish exposed to comprehensive suite of halogenated and organophosphate flame retardants, *Toxicol. Sci.* 145 (2015) 177–195, <https://doi.org/10.1093/toxsci/kfv044>.
- [17] D. Rhyu, H. Lee, R.L. Tanguay, K.-T. Kim, Tris(1,3-dichloro-2-propyl)phosphate (TDCIPP) disrupts zebrafish tail fin development, *Ecotoxicol. Environ. Saf.* 182 (2019) 109449, <https://doi.org/10.1016/j.ecoenv.2019.109449>.
- [18] R. Li, L. Zhang, Q. Shi, Y. Guo, W. Zhang, B. Zhou, A protective role of autophagy in TDCIPP-induced developmental neurotoxicity in zebrafish larvae, *Aquat. Toxicol.* 199 (2018) 46–54, <https://doi.org/10.1016/j.aquatox.2018.03.016>.
- [19] R. Li, P. Zhou, Y. Guo, B. Zhou, The involvement of autophagy and cytoskeletal regulation in TDCIPP-induced SH-SY5Y cell differentiation, *Neurotoxicology* 62 (2017) 14–23, <https://doi.org/10.1016/j.neuro.2017.05.002>.
- [20] Y. Zhao, W. Liu, D. Zhang, J. Shen, X. Huang, L. Xiao, et al., Association between organophosphorus flame retardants exposure and cognitive impairment among elderly population in southern China, *Sci. Total Environ.* 848 (2022) 157763, <https://doi.org/10.1016/j.scitotenv.2022.157763>.
- [21] C. Zou, T. Yang, J. Zhang, X. Chen, J. Zhao, D. Wu, et al., A quantitative proteomic study reveals oxidative stress and synapse-related proteins contributed to TDCIPP exposure induced neurotoxicity, *Ecotoxicol. Environ. Saf.* 271 (2024) 116005, <https://doi.org/10.1016/j.ecoenv.2024.116005>.
- [22] J. Root, P. Merino, A. Nuckols, M. Johnson, T. Kukar, Lysosome dysfunction as a cause of neurodegenerative diseases: lessons from frontotemporal dementia and amyotrophic lateral sclerosis, *Neurobiol. Dis.* 154 (2021) 105360, <https://doi.org/10.1016/j.nbd.2021.105360>.
- [23] B. Xu, C. Zheng, X. Chen, Z. Zhang, J. Liu, P. Spencer, et al., Dysregulation of myosin complex and striated muscle contraction pathway in the brains of ALS-SOD1 model mice, *ACS Chem. Neurosci.* 10 (2019) 2408–2417, <https://doi.org/10.1021/acschemneuro.8b00704>.
- [24] L. Wu, P. Rosa-Neto, G.-Y.R. Hsiung, A.D. Sadovnick, M. Masellis, S.E. Black, et al., Early-onset familial Alzheimer's disease (EOFAD), *Can. J. Neurol. Sci.* 39 (2012) 436–445, <https://doi.org/10.1017/s0317167100013949>.
- [25] H. Hampel, R. Vassar, B. De Strooper, J. Hardy, M. Willem, N. Singh, et al., The β -secretase BACE1 in alzheimer's disease, *Biol. Psychiatr.* 89 (2021) 745–756, <https://doi.org/10.1016/j.biopsych.2020.02.001>.

- [26] Q. Zhou, X. Fu, X. Wang, Q. Wu, Y. Lu, J. Shi, et al., Autophagy plays a protective role in Mn-induced toxicity in PC12 cells, *Toxicology* 394 (2018) 45–53, <https://doi.org/10.1016/j.tox.2017.12.001>.
- [27] X. Zhang, M. Wei, J. Fan, W. Yan, X. Zha, H. Song, et al., Ischemia-induced upregulation of autophagy precludes dysfunctional lysosomal storage and associated synaptic impairments in neurons, *Autophagy* 17 (2021) 1519–1542, <https://doi.org/10.1080/15548627.2020.1840796>.
- [28] Y.C. Kim, K.-L. Guan, mTOR: a pharmacologic target for autophagy regulation, *J. Clin. Invest.* 125 (2015) 25–32, <https://doi.org/10.1172/JCI73939>.
- [29] Z. Zhu, C. Yang, A. Iyaswamy, S. Krishnamoorthi, S.G. Sreenivasmurthy, J. Liu, et al., Balancing mTOR signaling and autophagy in the treatment of Parkinson's disease, *Int. J. Mol. Sci.* 20 (2019) 728, <https://doi.org/10.3390/ijms20030728>.
- [30] J.A. Fielhaber, Y.-S. Han, J. Tan, S. Xing, C.M. Biggs, K.-B. Joung, et al., Inactivation of mammalian target of rapamycin increases STAT1 nuclear content and transcriptional activity in alpha4- and protein phosphatase 2A-dependent fashion, *J. Biol. Chem.* 284 (2009) 24341–24353, <https://doi.org/10.1074/jbc.M109.033530>.
- [31] L. Yang, N. Li, D. Yang, A. Chen, J. Tang, Y. Jing, et al., CCL2 regulation of MST1-mTOR-STAT1 signaling axis controls BCR signaling and B-cell differentiation, *Cell Death Differ.* 28 (2021) 2616–2633, <https://doi.org/10.1038/s41418-021-00775-2>.
- [32] E. Butturini, A. Carcereri de Prati, S. Mariotto, Redox regulation of STAT1 and STAT3 signaling, *Int. J. Mol. Sci.* 21 (2020) 7034, <https://doi.org/10.3390/ijms21197034>.
- [33] A.A. Goldberg, B. Nkengfack, A.M.J. Sanchez, N. Moroz, S.T. Qureshi, A.E. Koromilas, et al., Regulation of ULK1 expression and autophagy by STAT1, *J. Biol. Chem.* 292 (2017) 1899–1909, <https://doi.org/10.1074/jbc.M116.771584>.
- [34] S. Levano, D. Bodmer, Loss of STAT1 protects hair cells from ototoxicity through modulation of STAT3, c-Jun, Akt, and autophagy factors, *Cell Death Dis.* 6 (2015) e2019, <https://doi.org/10.1038/cddis.2015.362>.
- [35] A.M. Cataldo, D.J. Hamilton, J.L. Barnett, P.A. Paskevich, R.A. Nixon, Properties of the endosomal-lysosomal system in the human central nervous system: disturbances mark most neurons in populations at risk to degenerate in Alzheimer's disease, *J. Neurosci.* 16 (1996) 186–199, <https://doi.org/10.1523/JNEUROSCI.16-01-00186.1996>.
- [36] S. Ghavami, S. Shojaei, B. Yeganeh, S.R. Ande, J.R. Jangamreddy, M. Mehrpour, et al., Autophagy and apoptosis dysfunction in neurodegenerative disorders, *Prog. Neurobiol.* 112 (2014) 24–49, <https://doi.org/10.1016/j.pneurobio.2013.10.004>.
- [37] S. Sjödin, G. Brinkmalm, A. Öhrfelt, L. Parnetti, S. Paciotti, O. Hansson, et al., Endo-lysosomal proteins and ubiquitin CSF concentrations in Alzheimer's and Parkinson's disease, *Alzheimer's Res. Ther.* 11 (2019) 82, <https://doi.org/10.1186/s13195-019-0533-9>.
- [38] H. Xu, M. O'Reilly, G.S. Gibbons, L. Changolkar, J.D. McBride, D.M. Riddle, et al., In vitro amplification of pathogenic tau conserves disease-specific bioactive characteristics, *Acta Neuropathol.* 141 (2021) 193–215, <https://doi.org/10.1007/s00401-020-02253-4>.
- [39] J. Domert, S.B. Rao, L. Agholme, A.-C. Brorsson, J. Marcusson, M. Hallbeck, et al., Spreading of amyloid- β peptides via neuritic cell-to-cell transfer is dependent on insufficient cellular clearance, *Neurobiol. Dis.* 65 (2014) 82–92, <https://doi.org/10.1016/j.nbd.2013.12.019>.
- [40] M.-H. Cho, K. Cho, H.-J. Kang, E.-Y. Jeon, H.-S. Kim, H.-J. Kwon, et al., Autophagy in microglia degrades extracellular β -amyloid fibrils and regulates the NLRP3 inflammasome, *Autophagy* 10 (2014) 1761–1775, <https://doi.org/10.4161/auto.29647>.